DOI: 10.13009/EUCASS2017-180

Implementation of Approximate Ablation Model in Aerodynamic Heating Prediction Tool

Buğra ŞİMŞEK, Sıtkı USLU*, Bayındır KURAN**, Mehmet Ali AK***
**TOBB University of Economics and Technology*
Söğütözü Caddesi No 43, 06560, Ankara, TURKEY
***Roketsan Missiles Industries Inc.*
Şehit Yüzbaşı Adem Kutlu Sokak, No 21, 06780 Elmadağ, TURKEY

Abstract

One dimensional computer code has been developed to calculate transient surface recession rates of ablative type thermal protection system of a supersonic vehicle. An approximate recession method that uses heat of ablation has been coupled to the aerodynamic heating prediction tool that calculates the in-depth thermal response. Trajectory data is used to calculate boundary conditions at the ablating surface. Blowing effect of the ablation on the aerodynamic heating is also considered. In-depth thermal response and surface recession rates are calculated as a function of time by use of explicit finite difference methodology. In-depth solution accounts for material decomposition, but does not account for pyrolysis gas energy absorption through the material. Conservation of energy is taken into account to derive governing equations and material properties are used as a function of temperature. An Arrhenius like equation is used to model the density of the ablative material. Verification of the recession rates and temperature calculations are performed in comparison with available test data from the literature and results of commercially available software.

Nomenclature

B_i	=	pre-exponential factor for the i^{th} resin component
C_p	=	specific heat of the material
E_{ai}	=	activation energy for the i^{th} resin component
$\dot{E}_{in}$	=	energy inflow to the structure
$\dot{E}_{out}$	=	energy outflow from the structure
$\dot{E}_{st}$	=	the rate change of thermal energy stored by the structure
h	=	heat transfer coefficient
i	=	time point
k	=	thermal conductivity
k*	=	thermal conductivity evaluated at the reference temperature
$\dot{m}$	=	mass injection rate
M_L	=	Local Mach number
n	=	number of nodes
Nu	=	Nusselt number
Nu_x	=	Nusselt number at a position x.
R	=	universal gas constant
Re	=	Reynolds number
Re_x	=	Reynolds number at a position x
q''_{hw}	=	hot wall heat flux
Q*	=	heat of ablation
r	=	recovery factor
$\dot{s}$	=	recession rate
St	=	Stanton number
t	=	time
T	=	temperature

DOI: 10.13009/EUCASS2017-180

T_L = local temperature
T_w = wall temperature
T^* = Eckert's reference temperature
u_e = boundary layer edge velocity
x = distance to point of interest from the leading edge/nose tip
γ = specific heat ratio of flow
δ = thickness of the insulation
ε = emissivity
Δx = distance between the nodes
Δt = time step size
Γ = resin volume fraction
ρ = density
ρ_{0i} = original density of the i^{th} resin component
ρ_{ri} = residual density of the i^{th} resin component
ρ_i = current density of the i^{th} resin component
σ = Stefan-Boltzman constant
ψ_i = density exponent factor

1. Introduction

At supersonic and hypersonic velocities large amount of kinetic energy is converted to thermal energy by viscous dissipation and a strong shock wave is formed in front of the nose cone and leading edges of the vehicle. These two phenomena increase the gas temperature around the body yielding aerodynamic heating in the form of forced convection. Structural parts and electronic devices of the vehicle have limited operating temperatures; therefore, it is compulsory to minimize the heat conducted into the body to prevent failure of the vehicle under aerodynamic heating.

Thermal protection systems minimize the heat conducted into the body by insulating the vehicle. Ablation is one of the most widely used processes on the thermal protection systems. In this process, energy is rejected from the body by mass loss. Mass loss can be achieved by phase change, decomposition or chemical erosion. During these processes, energy is absorbed; therefore, energy conducted into the body is reduced. Moreover, mass injection into the boundary layer reduces the aerodynamic heating in consequence of blockage effect.

Thickness of the insulation is very critical for the thermal design of the vehicle. Inadequate thickness may cause the vehicle to fail at the mission due to high level of temperature or recession. Larger thickness increase cost and weight, which is undesired. As a result, optimum thickness of the ablative material should be determined at the design phase of high-speed air vehicles. Consequently, design of an external insulation system requires a deep evaluation of the flight conditions to fit best compromise between ablation effectiveness and design constraints.

An approximate ablation model is implemented into the aerodynamic heating prediction tool to predict the thermal performance of ablative type insulation materials in preliminary design phase. The complex chemical phenomena occurring during ablation are numerically modelled assuming simplifying hypotheses reported in literature. By this tool, it is possible to obtain rapid estimates with reasonably accurate results with much less running time. Details of the aerodynamic heating tool are given in [1]. Theoretical background and procedures for calculating the recession histories are presented in the following sections. In addition to verification studies given in [1], one more study is also conducted to check the accuracy of the aerodynamic heating prediction tool by CFD simulations.

2. Theoretical Background

2.1 Governing Equations

A simple one-dimensional equation under transient conditions with constant properties and without internal generation is given in Eq. (1). This equation is solved with explicit time stepping and finite differences in space to calculate temperature distribution in the thermal protection system and structure.

$$\frac{1}{\alpha}\frac{\partial T}{\partial t} = \frac{\partial^2 T}{\partial y^2} \tag{1}$$

DOI: 10.13009/EUCASS2017-180

Heat transfer equation for the convective aerodynamic heating and surface radiation can be written as given in Eq. (2). This equation is used as boundary condition for the outer nodal point.

$$q'' = h(T_r - T_w) - \sigma\varepsilon(T_w^4 - T_\infty^4) \tag{2}$$

Recovery temperature is the maximum temperature in the boundary layer and it is mathematically expressed as:

$$T_r = T_L\left(1 + r\frac{\gamma - 1}{2}M_L^2\right) \tag{3}$$

Eckert reference temperature approach is followed to compute heat transfer coefficient. This method is approximate with reasonable accuracy. In this approach temperature-related transport and thermodynamic properties in the classical incompressible formulae expressions are evaluated at a reference temperature (T*) which is given in Eq.4 [2].

$$T^* = T_L + 0.5(T_w - T_L) + 0.22(T_r - T_L) \tag{4}$$

For flow over a flat plate, the Nusselt Number for laminar and turbulent flows as a function of Reynolds and Prandtl numbers are given below respectively [3]:

$$Nu_x = 0.33206\sqrt{Re_x}(Pr)^{\frac{1}{3}} \ ; \text{laminar flows} \tag{5}$$

$$Nu_x = 0.02914(Re_x)^{\frac{4}{5}}(Pr)^{\frac{1}{3}} \ ; \text{turbulent flows} \tag{6}$$

where

$$Nu_x = \frac{hx}{k^*} \tag{7}$$

For the points on the conical side, the heat transfer coefficient is multiplied by a factor and then calculation is done as for a flat plate. For the conical side, there is a three-dimensional relieving effect that resulting in thinner boundary layer. This in turn results in larger velocity and temperature gradient in the boundary layer and hence causes a higher heat transfer. Laminar to turbulent transition is taken into account buy use of transition criteria based on the Reynolds number and other details of the aerodynamic heating prediction tool are given in [1].

2.2 Calculation of Surface Recession

Steady state ablation approach employing heat of ablation, Q*, is implemented into the tool by using Eq.8 [4]. Surface recession is calculated and thickness of the thermal protection system is updated at every step for the in-depth temperature calculations.

$$\dot{s} = \frac{q''_{hw}}{\rho Q^*} \tag{8}$$

Equation 8 is conservative and will generally over predict the actual recession rate. This over prediction will grow as material density decreases and the heat rate increases. To correct for this over prediction, a recession threshold temperature can be incorporated, below which the recession rate is set to zero [4].

2.3 Blowing Correction of Heat Transfer Coefficient

Mass injection into boundary layer during ablation decreases net heat flux into surface. Injection process thickens the boundary layer which results in a decrease in the velocity and temperature gradient adjacent to the vehicle wall. In the tool decrease in the heat transfer coefficient due to blowing is calculated by Eq.9.

$$\eta = \frac{h_{blown}}{h_{unblown}} = \frac{\Phi}{e^{\Phi} - 1} \tag{9}$$

where

DOI: 10.13009/EUCASS2017-180

$$\Phi = \frac{2\lambda \dot{m}}{\rho_e u_e St_{unblown}} \tag{10}$$

In Eq. 10 λ is the empirical blowing rate parameter and usually is it recommended as 0.5 for the laminar flows and 0.4 for the turbulent flows.

2.4 TPS Material Density

The change in the density as a function of temperature is computed using the Arrhenius like equation which is given in Eq. 11. This formulation uses a three-component model for the density decomposition and the material density ρ can be obtained as the weighted mean of its components as given in Eq.12., [4]. Γ is the resin volume fraction, 1 and 2 represent the resin components and 3 represents reinforcement fiber. Other coefficients can be determined by termogravimetry analysis (TGA).

$$\frac{\partial \rho_i}{\partial t} = -\left(B_i e^{\frac{E_i}{RT}}\right) \rho_{0i} \left(\frac{\rho_i - \rho_{ri}}{\rho_{oi}}\right)^{\psi_i} \quad i = 1,2,3 \tag{11}$$

$$\rho = \Gamma(\rho_1 + \rho_2) + (1 - \Gamma)\rho_3 \tag{12}$$

Equation 11 is explicitly solved in the tool to calculate density of the ablative material as a function of temperature and time. Calculated density is used in Eq.8 to predict recession rates and used in Eq.14 to compute temperatures.

3. Finite Difference Approach

Mathematical equations are derived for the nodes which are represented in Fig.1. An equal spacing between the nodes is used as an input parameter and it is checked according to stability concerns.

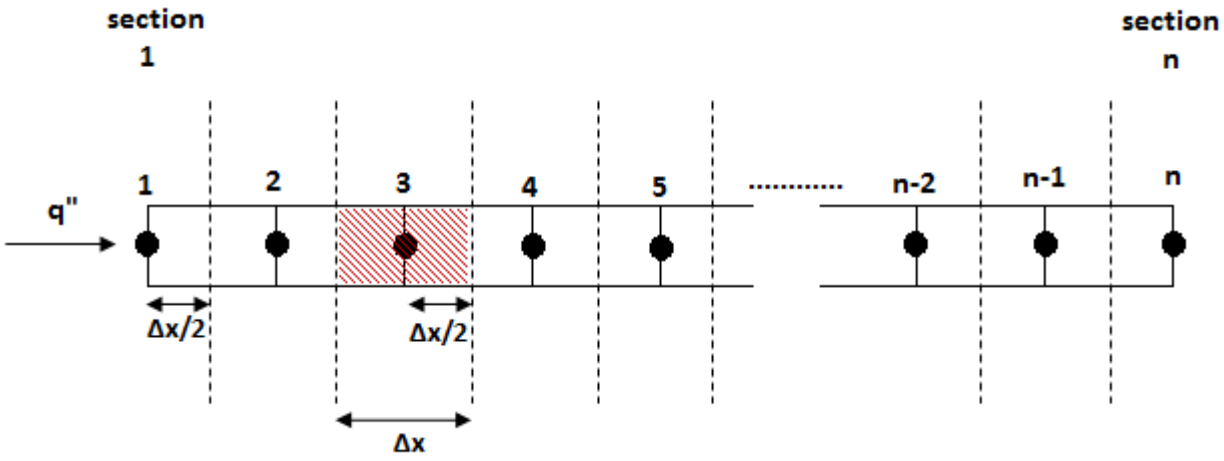

Figure 1: Representation of the nodes in the tool and details of third section.

For each node conservation of energy equation given in Eq. 13 is used to derive governing equations that will be explicitly discretized. The derivation is lengthy and for an interior node at section 3, discretized governing equation is given in Eq.14. Material properties are used as a function of temperature; therefore these properties are also calculated at each time step. Linear interpolation is performed to find material properties at the corresponding nodal temperatures. For the node at the outer surface, aerodynamic heating and radiation are used in the inlet energy term of Eq. 13. Calculation steps for the mesh size and insulation thickness are given in Eq.15 and Eq.16.

DOI: 10.13009/EUCASS2017-180

$$\dot{E}_{in} - \dot{E}_{out} = \dot{E}_{st} \tag{13}$$

$$k_2^i \frac{T_2^i - \left(\frac{T_2^i + T_3^i}{2}\right)}{\Delta x/_2} - k_3^i \frac{T_3^n - \left(\frac{T_3^i + T_4^i}{2}\right)}{\Delta x/_2} = \Delta x^i \rho_3^i Cp_3^i \frac{T_3^{i+1} - T_3^i}{\Delta t} \tag{14}$$

$$\delta^{i+1} = \delta^i - \dot{s}\Delta t \tag{15}$$

$$\Delta x^i = \frac{\delta^i}{n-1} \tag{16}$$

$$k_n^i = f_1(T_n^i) \;\; ; \;\; Cp_n^i = f_2(T_n^i) \;\; ; \;\; \rho_n^i = f_3(T_n^i, t) \tag{17}$$

4. Validation of the Tool

Four different validation studies are performed. In the first one, an additional validation of the aerodynamic heating tool without ablation is made. Previous validation studies are given in [1] in detail. In the second one, implemented interpolation subroutines for the temperature related material properties are validated. The first version of the aerodynamic heating tool uses constant material properties for the insulation and structure; therefore with this study tool is also enhanced in this aspect. In the third one tool is validated under constant recession rates and in the fourth one, tool is used to predict temperatures under reference test conditions and results are compared with the test data found in the literature.

4.1 Validation Study 1

In this validation study, an axisymmetric, transient conjugate heat transfer analysis is made by use of a CFD tool. A generic shape blunt body which is given Fig.2 is used. Material of the body is aluminium and properties of the material are taken constant. Velocity profile is given in Fig.3. Free stream temperature and pressure are taken constant as 300 K and 101325 Pa. Spalart-Allmaras turbulence model is used in the simulation. Dimensions of the overall planar solution domain are 10000 mm height and 18400 mm width.

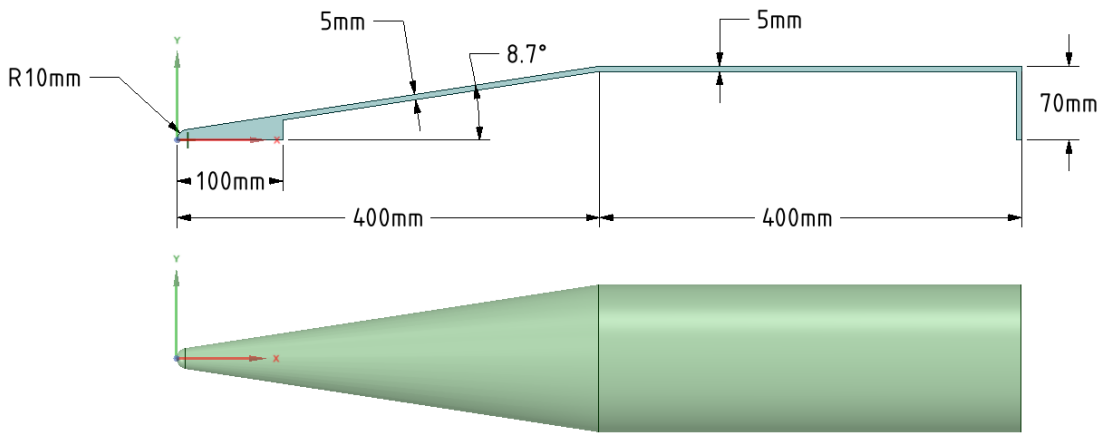

Figure 2: General dimensions of blunt body

DOI: 10.13009/EUCASS2017-180

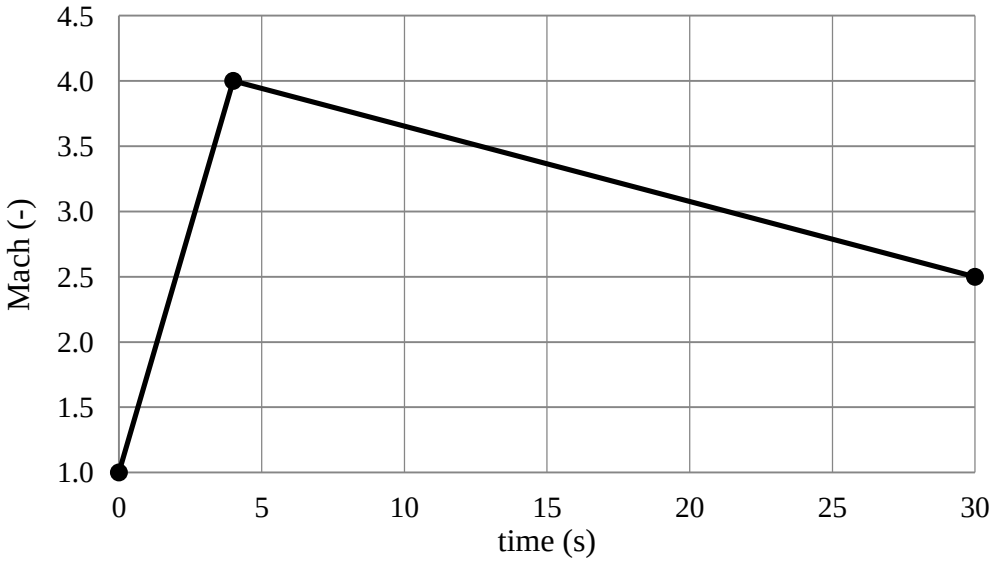

Figure 3: Velocity profile

Solution domain is created by polygonal and prism layer meshers. Number of 30 prism layers are used on the walls with 1.1 growth rate and first prism layer thickness is used as 0.06 mm. Due to computational CPU requirements finer mesh domain was not preferred. General views of solution domain are given in Fig 4. and Fig.5.

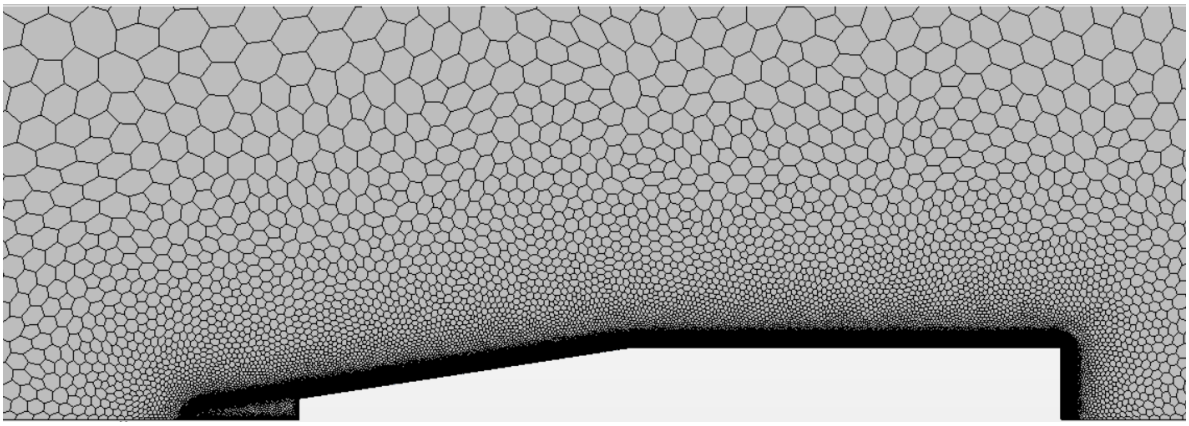

Figure 4: General view of solution domain-1

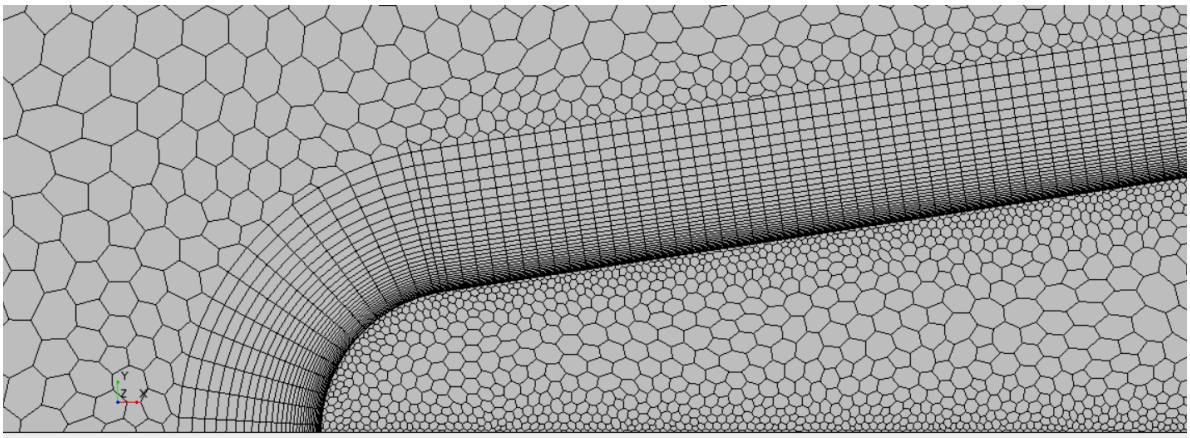

Figure 5: General view of solution domain-2

DOI: 10.13009/EUCASS2017-180

Results of two points, point 1 and point 2, located on the conical and horizontal sides of the body are compared. Locations of the point 1 and point 2 are given in Fig.6.

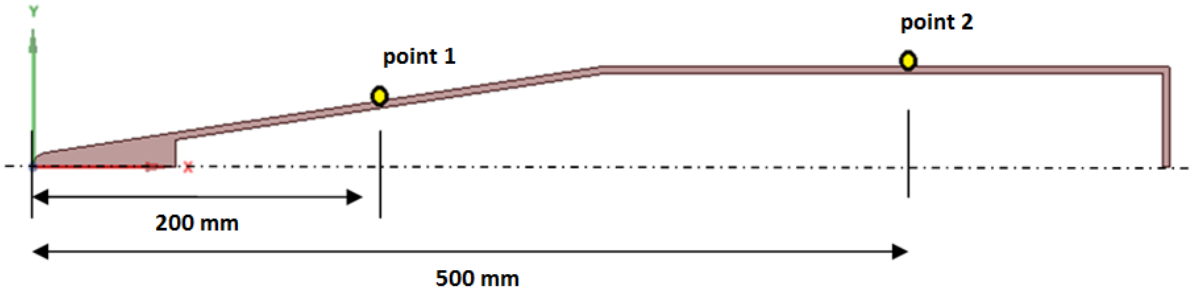

Figure 6: Locations of point 1 and point 2 on the body

Comparisons of the temperatures found by CFD simulation and prediction tool are given Fig 7. As seen in Fig.7 differences between the simulated and predicted results are less than 5%. Considering the time consuming process of CFD simulations, calculation of temperatures within 5% error in only a few seconds is very advantageous during preliminary design phase. Temperature distributions at the specific time are given in Fig.8 and Fig.9.

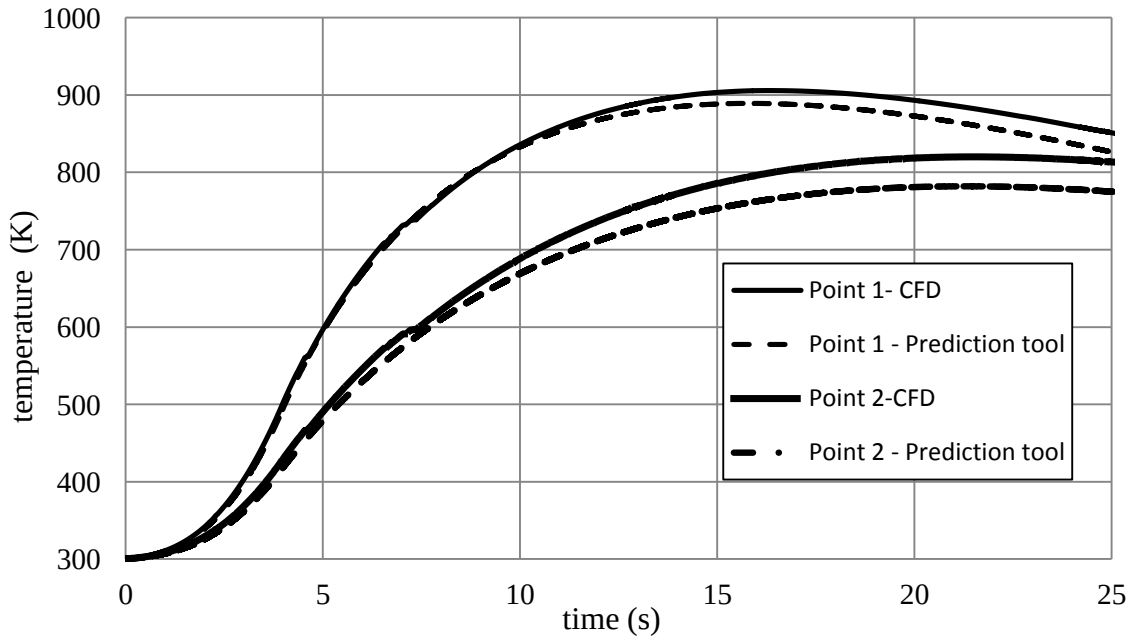

Figure 7: Comparison of simulated and predicted temperatures of point 1 and point 2

DOI: 10.13009/EUCASS2017-180

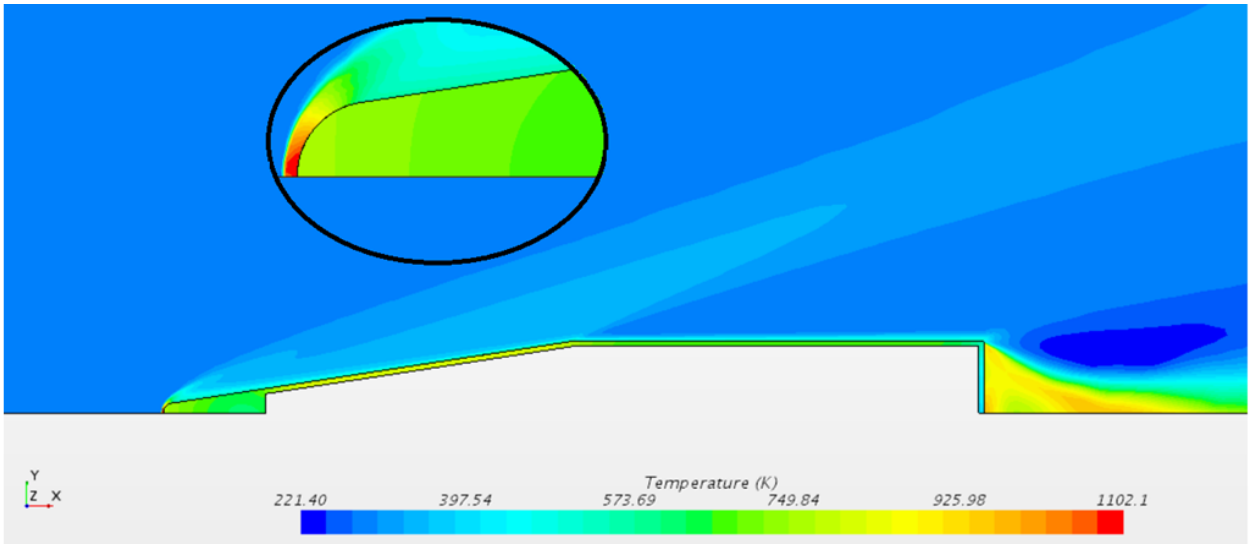

Figure 8: Temperature Distribution at t=9.5s.

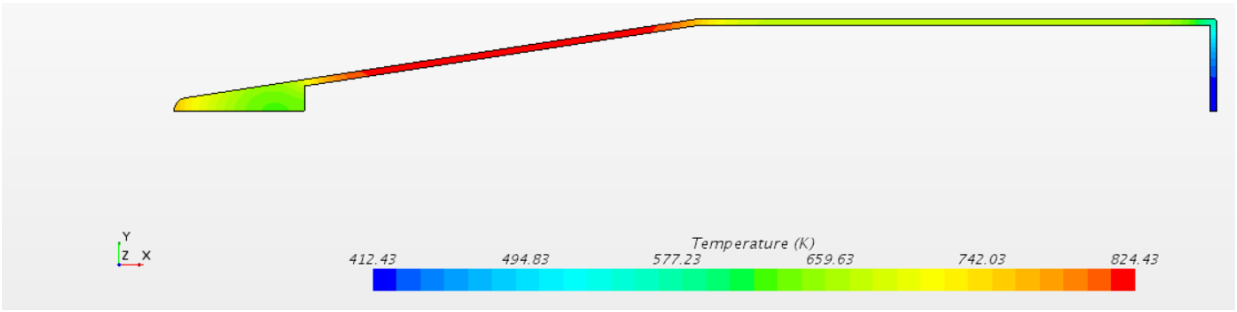

Figure 9: Temperature Distribution on the Body at t=9.5s

4.2 Validation Study 2

In the second validation study, under time dependent convective heat flux, temperature histories of the outer and inner surfaces are calculated. For the insulation material, temperature dependent conductivity and specific heat capacity are used. There is no ablation. Purpose of this validation study is to check the interpolation subroutines calculating the nodal material properties at corresponding nodal temperatures. As mentioned before, in the first version of the aerodynamic heating prediction tool constant material properties were used. Tool is also enhanced with this respect in this study. Schematic representation of the problem is given in Fig.10.

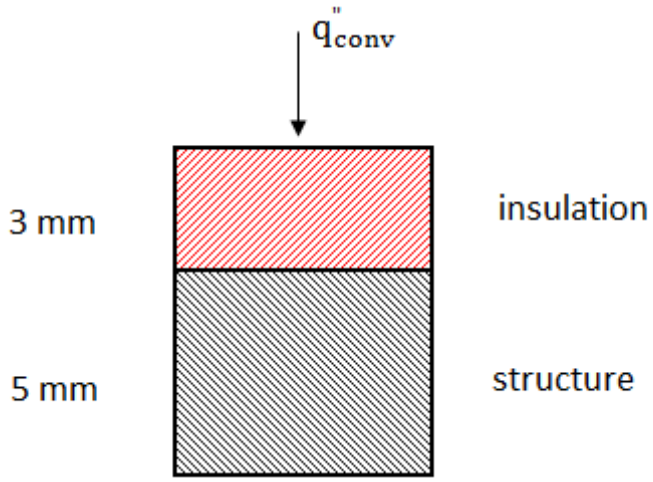

Figure 10: Representation of problem

DOI: 10.13009/EUCASS2017-180

Time dependent heat transfer coefficient and reference temperature are given in Fig.11 and material properties of the insulation material are given in Fig.12. Properties of the structure and density of the insulation are taken constant and material of the structure is aluminium. Thermal analysis is conducted by use of commercially available FEA software and results of the inner and outer points are compared in Fig 13. Initial temperature of the problem is 290 K.

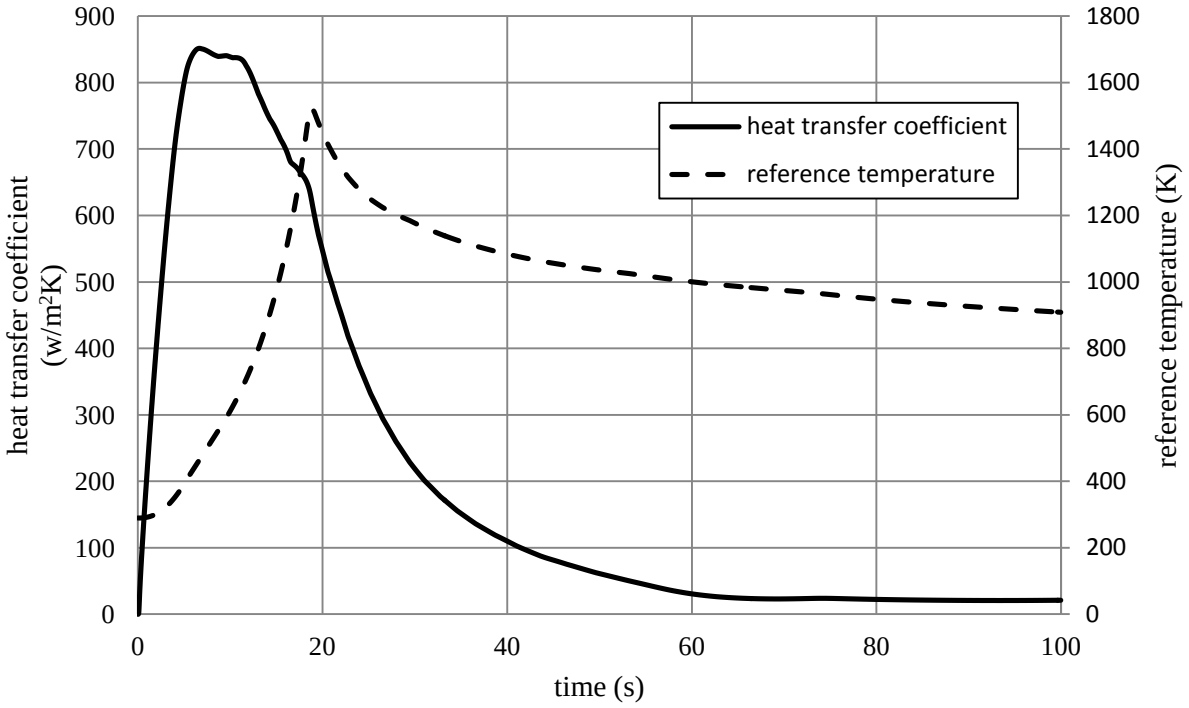

Figure 11: Convective boundary conditions of validation study 2

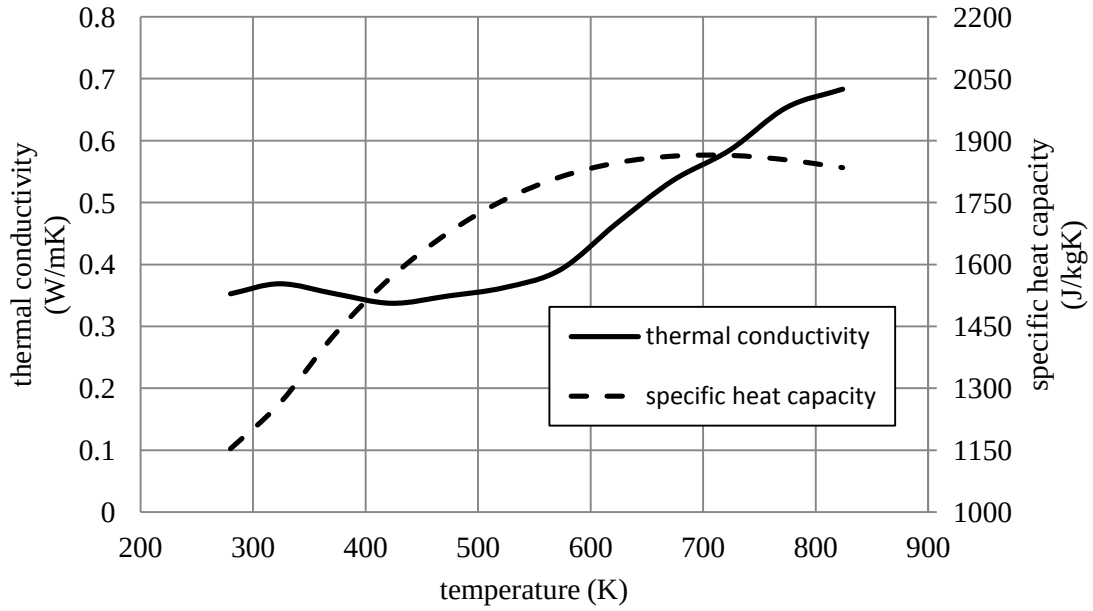

Figure 12: Material properties of insulation

DOI: 10.13009/EUCASS2017-180

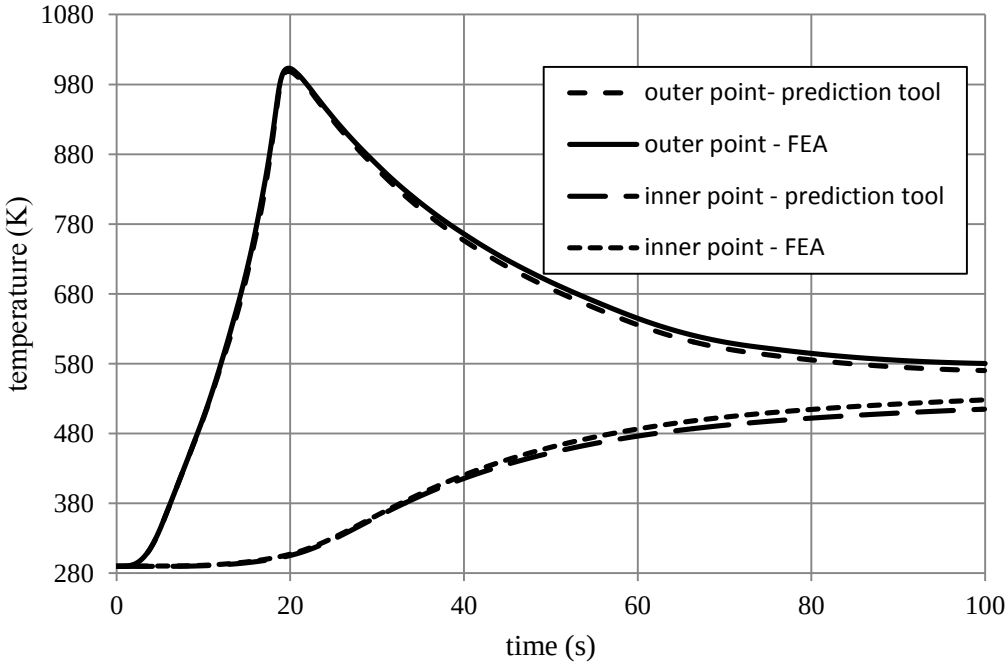

Figure 13: Comparison of outer and inner surface temperatures

As seen in Fig.13, results of prediction tool are found to be in good agreement with results of finite element analysis. These results are show that implementation of subroutines to use temperature related material properties in the prediction tool are achieved.

Validation Study 3

In the third validation study, in-depth temperature calculation is conducted under constant surface recession rate and heating rates. Geometry of the second validation study is used with same material properties. Applied recession rate is 0.02 mm/s and heat flux is 10000 W/m^2. Inner surface is assumed as adiabatic. Analysis is conducted by use of prediction tool and ablation module of MSC MARC. General representation of FEA model is given in Fig.14.

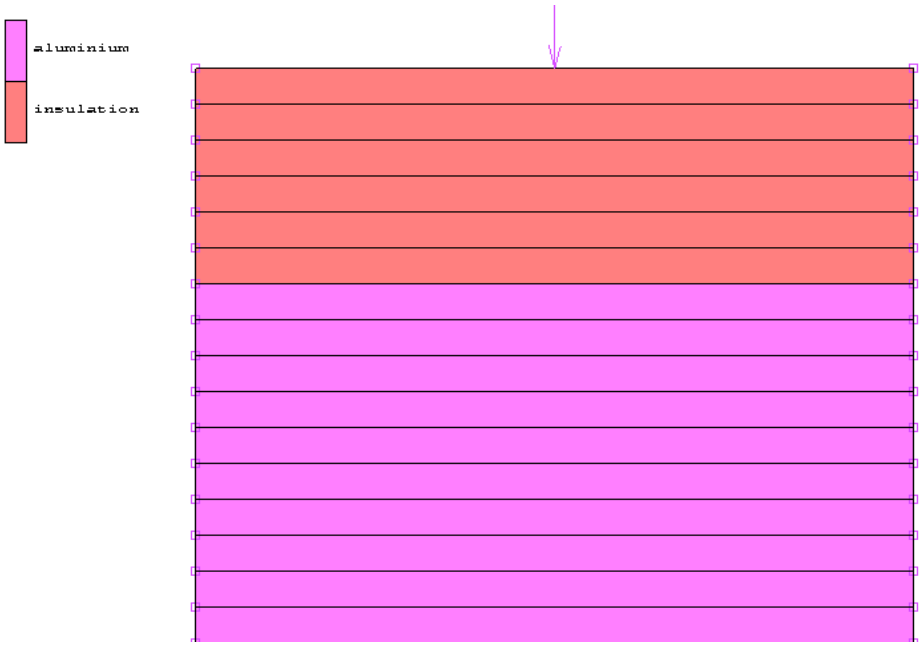

Figure 14: Representation of FEA model of validation study 3

DOI: 10.13009/EUCASS2017-180

Analysis is done for 50 seconds and temperature distributions at the initial and at the end of the analysis are given in Fig.15. Total recession is 1 mm. Shaver remeshing technique is used for the insulation.

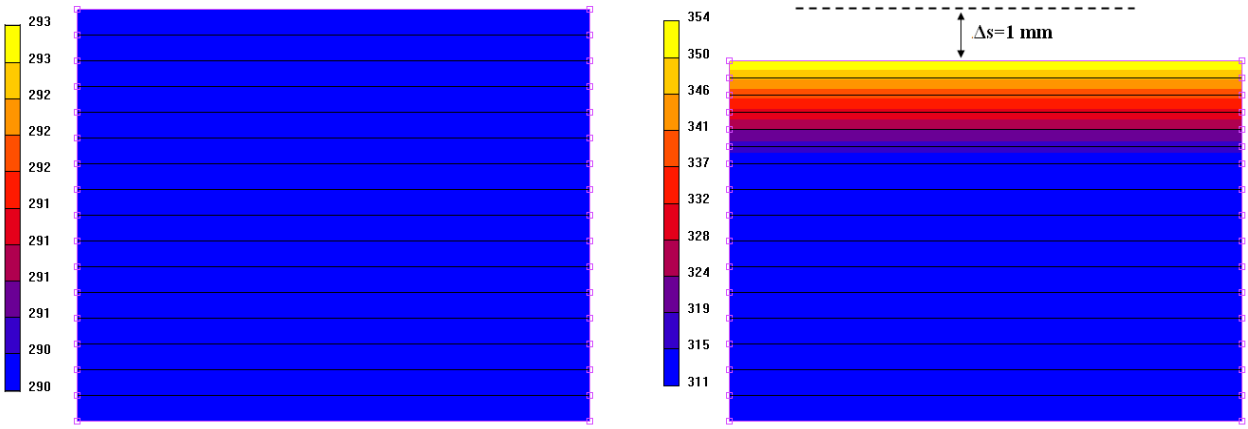

Figure 15: Initial and final temperature distribution at the insulation and structure

By use of same boundary conditions and material properties and thickness values simulation is done by use of prediction tool. Comparisons of the results are given in Fig 16. As seen in the figure results compare well and it is concluded that prediction tool is also validated under constant recession rates.

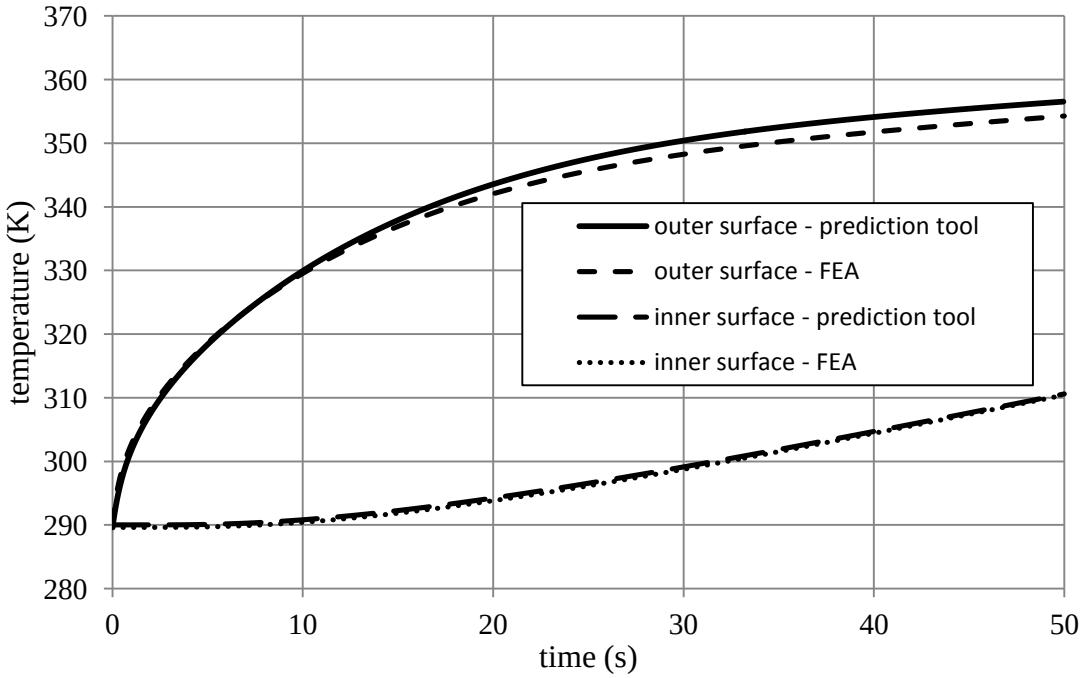

Figure 16: Comparison of outer and inner surface temperatures

DOI: 10.13009/EUCASS2017-180

Validation Study 4

In the fourth validation study, numerical results are crosschecked with outcomes of experimental tests reported in [6]. Test conditions and material properties are taken from [5].

Table 1: Test condition for model verification [5]

q''_{cw} [MW/m^2]	P[atm]	H_{tot} [MJ/kg]	t_{max} [s]
5.80	0.45	29.5	15

Initial height of 27.4 mm has been used in the analysis. In-depth response of the material has been calculated by use of prediction tool. The main approaches are given below:

- Initial temperature of 300 K is considered.
- 1-d simulation has been carried out with time step size of 0.001 seconds.
- An adiabatic condition has been applied to the bottom surface.
- Thermal conductivity and specific heat capacity of the material has been used as a function of temperature.
- Density of the material has been calculated by means of Arrhenius like equation.
- Heat of ablation of the material is taken as a function of hot wall convective heat flux.
- A hot wall convective heat flux and re-radiated heat flux has been applied on the top surface.
- Blowing correction for convective heat flux has been taken into account.

Comparison between the numerical and experimental temperature profiles for the top surface is given in Fig 17. It is clear that prediction tool seems to be sufficiently accurate when compared with a validated numerical tool proposed in the literature [5] and labelled as "Covington". Maximum error between the numerical and test result is nearly 15% and cause of the errors are explained in detail in [6]. Comparison between numerical and experimental results is given in Table 2. The error between post-test thicknesses is nearly 4.2%. The assumption of one-dimensional heat transfer in the numerical analysis is one of the main sources of the error.

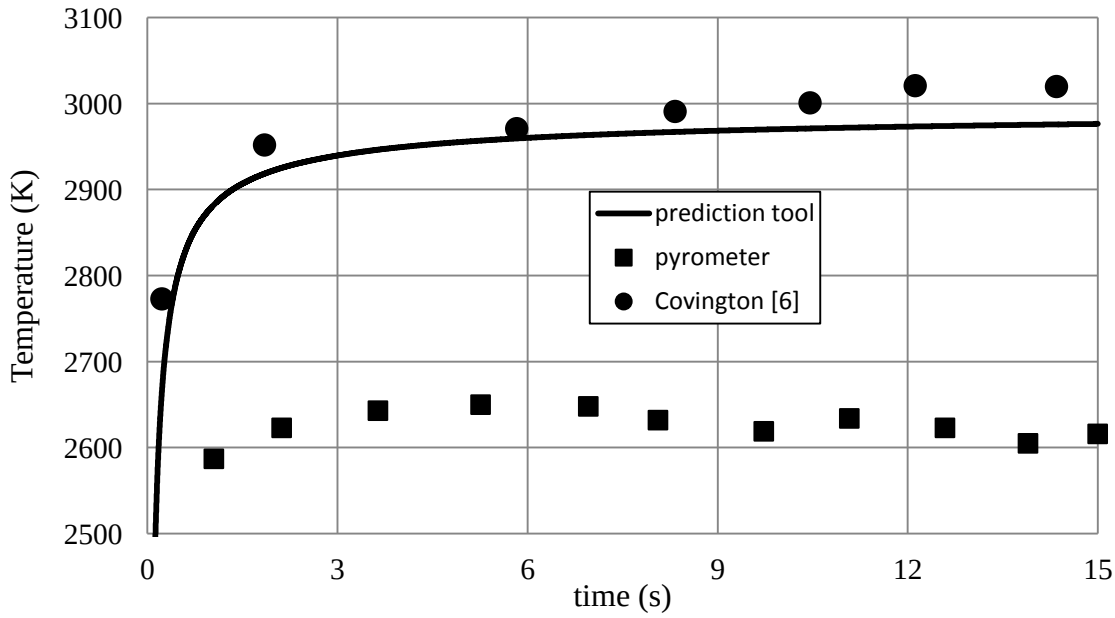

Figure 17: Comparison among the numerical and experimental surface temperature profiles

DOI: 10.13009/EUCASS2017-180

Table 2: Comparison of Numerical and Experimental Recessions

	Initial height (mm)	**Final height (mm)**	**Total recession (mm)**	**Error on final height (-)**
Numerical	27.4	24.9	2.5	4.2%
Experimental [5]	27.4	26.0	1.4	--

5. Conclusions

An explicit numerical approach for ablation modelling has been developed and implemented in an aerodynamic heating prediction tool. Material properties are taken into account as a function of temperature. By use of a flight trajectory, aerodynamic heating and corresponding surface ablation are calculated in a single transient simulation. Four different validation studies have been performed and it is concluded that tool is very effective and accurate and can be used especially in the preliminary design phases. In the future it is planning to perform additional validation studies with different test conditions and material properties.
Tool can be used over a wide range of trajectories, materials and rapidly computes results that enable the user to easily investigate changes in material characteristics, insulation effectiveness and flight trajectories without having to employ more complex calculations.

References

[1] Simşek B.,Kuran B., Ak M.A., Uslu S.,2016. Aerodynamic Heating Prediction Tool for a Supersonic Vehicle for Conceptual Design Phase. In :*46th AIAA Thermophysics Conference*
[2] Bertin, J.J., Hypersonic Aerothermodynamics, *AIAA Education Series*, AIAA, Washington, 1994, Chaps.1, 7
[3] Arnas, A. Ö., Daisie, D. B., Gunnar, T., Seth, A.N., Jason, R.W., Michael, J. B., Bret, P. V., On the Analysis of the Aerodynamic Heating Problem, Journal of Heat Transfer, Vol. 132, No.12, 2010.
[4] Dec, J.A., and Braun R.D., An Approximate Ablative Thermal Protection System Sizing Tool for Entry System Design, 44th AIAA Aerospace Sciences Meeting and Exhibit, , Reno, Nevada, AIAA 2006-780, Jan. 2006.
[5] Carandente V.,Scigliano R., Simone V.D.,Vecchio A.D.,Gardi R., A Finite Element Approach for the Design of Innovatıve Ablative Materials for Space Applications, 2015. In: *6th European Conference for Aeronautics and Space Sciences (EUCASS)*
[6] Covington, M.A. 2004. Performance of a Light-Weight ablative thermal protection material for the StardustMission sample return capsule. In: *2nd International Planetary Probe Workshop.*